Autocatalytic reaction networks in bioinspired systems

Theses of doctoral (PhD) dissertation

Emese Lantos

Supervisor: **Dr. Ágota Tóth**, *full professor*

Doctoral School of Chemistry

University of Szeged, Department of Physical Chemistry and Materials Science

2023

1 Introduction and Aims

The world around us is a group of complex systems that cannot be investigated and handled in detail by applying the tools of a single discipline but requires multidisciplinary research. Let us consider the physiological processes that take place in our bodies, the varying patterns of animals, the typical behaviours of animal populations, or even the processes occurring in space. We must not forget the Covid-19 pandemic, fundamentally shaking the last few years, or even global warming, which we need to handle with the tools of natural sciences.

Systems biology research, which has been spreading in recent decades, has made the demand for a new field of chemistry combining the frontier sciences: systems chemistry. The basic assumption of this discipline is that it oversteps from the level of single, individual molecules to the supramolecular level and it derives the new, apparent properties of the system from the interactions between particles. The scope of systems chemistry covers not only self-organization, self-assembly, and oscillating reactions but also molecular machines, and reaction networks. In addition, nonlinear dynamics must be mentioned, the results of which system chemistry relies heavily on.

The common features of the systems studied and modelled in my work are that they are biologically relevant and indicate non-linear chemical behaviour – autocatalysis and/or oscillation and/or pattern formation. In one case, we focused on an enzyme playing an important role in biology, while in the other case, we investigated a reaction network that is able to show oscillation around physiological pH.

In the beginning, we aimed to establish a relevant model to explain the characteristics of the front reaction experimentally observed in the hydrogenase enzyme – benzyl viologen system. After that, we focused on another reaction, the hydrolysis of Schiff bases, as the possibility of autocatalysis has been raised in the past. Based on the experimental and modelling results, it was shown that the hydrolysis of the tested compounds indicated autocatalysis, which could not be related to a specific reaction but to a reaction network involving several steps. The model, complemented with a general removal step, has been analysed in an open system, the results of which can be used and extended to other reactions to create targeted drug delivery or sensing systems in the future.

2 Experimental Section

Initially, the hydrolysis of Schiff bases was investigated in a beaker that served as a batch reactor by monitoring the pH change under constant stirring at a solvent ratio of 10-90 V/V% ethanol-water. During the measurements, the initial pH was systematically modified by adding an appropriate amount of hydrochloric acid, which removed the hydroxide ions acting as an autocatalyst in the reaction and ultimately allowed the determination of the strength of the autocatalysis. Later, I also investigated the strength of autocatalysis at other ethanol-water solvent ratios. The process was also monitored in an open system using a continuously stirred tank reactor made of poly(methyl methacrylate).

3 Modelling

Different software and software packages were used to solve ordinary differential equations. In well-stirred reactors, the governing equation describing the system is

$$\frac{dc_i}{dt} = f(c_i) + k_0(c_{i,0} - c_i), \tag{1}$$

where *f(c_i)* is the kinetic term, $k_0(c_{i,0} - c_i)$ is the flow term, $c_{i,0}$ is the inflow, and c_i is the outflow concentration of the ith component. These equations were solved by *CVODE*, and *XPPAUT* package, also based on this previous solver. The rate and equilibrium constants required for imine hydrolysis modelling were determined by fitting the experimental curves in *Copasi* using Levenberg-Marquardt's method. Subsequently, the bifurcation and oscillation of the resulting system were investigated using *AUTO*, the built-in programme of the *XPPAUT* software package.

The governing equation of the spatiotemporal behavior of the system is given by

$$\frac{\partial c_i}{\partial t} = D_i \frac{\partial^2 c_i}{\partial x^2} + f(c_i), \tag{2}$$

where the first half of the expression is describing the diffusion, while the second half is related to the reaction kinetics. The diffusion coefficient of the ith component is indicated with D_i and x is the spatial coordinate. We have considered literature and experimental data to model the reactions of the hydrogenase enzyme. The partial differential equations obtained from modelling the enzyme behaviour were further processed by using *CVODE*, BDF integrating routine from the *SUNDIALS* software package.

4 New Scientific Results

I. *By using our model for the hydrogenase–benzyl-viologen front-forming reaction, we have shown that at different total electron acceptor and total enzyme concentration ratios (**R=M_T/E_T**), two different reaction fronts emerge depending on the spatial and temporal separation of the autocatalytic step and the reduction of the electron acceptor* [3].

When an electron acceptor molecule, in this case benzyl viologen, was added to the hydrogenase enzyme under anaerobic conditions, it was observed that a reaction front was initiated spontaneously, which could be visually monitored by the purple colour of the reduced form of the electron acceptor. The reaction catalysed by the enzyme *HynSL* extracted from *Thiocapsa roseopersicina* can be described by the following equation:

$$H_2 + 2M \rightleftharpoons 2H^+ + 2M^-, \tag{3}$$

where the electron acceptor benzyl viologen nominated with M. Our model describing the hydrogenase–benzyl-viologen reaction is illustrated in Figure 1.

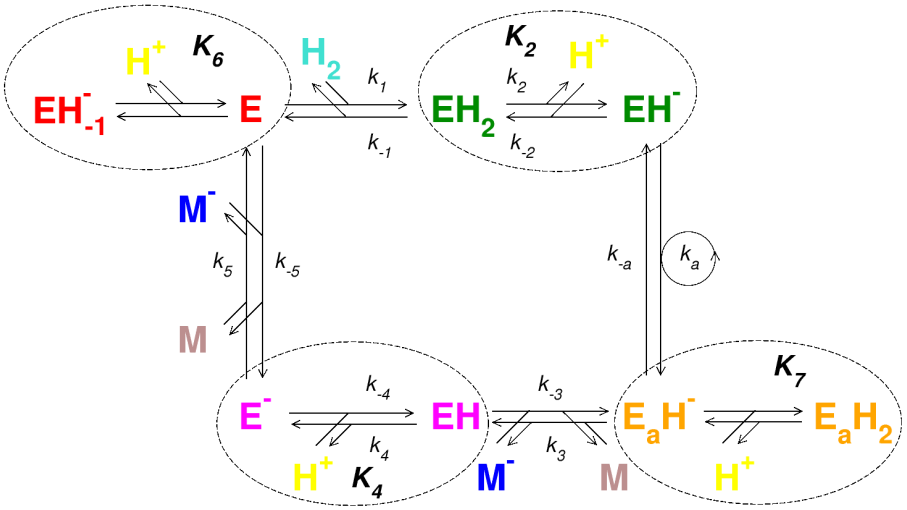

Figure 1: Schematic model of the hydrogenase enzyme reaction in the presence of benzyl viologen. E: free enzyme, EH^-_{-1} its deprotonated variant; EH_2: fully reduced enzyme, EH^-: its deprotonated form; E_aH^-: autocatalytic enzyme conformer, E_aH_2: protonated form of it; EH: partially reduced enzyme, E^-: its deprotonated form; M: electron acceptor; M^-: deprotonated form of it.

During the modelling, *R* was introduced as the ratio of the total electron acceptor and enzyme concentrations. If the electron acceptor is present in a large excess (Fig. 2. (a)), the emerging reaction-diffusion front appears sharp, and the autocatalytic and the reduction steps occur simultaneously. On the other hand, when the concentration of benzyl viologen is reduced (Fig. 2. (b)), the reduction step is much slower, resulting in a diffusive front and a spatially separated autocatalysis.

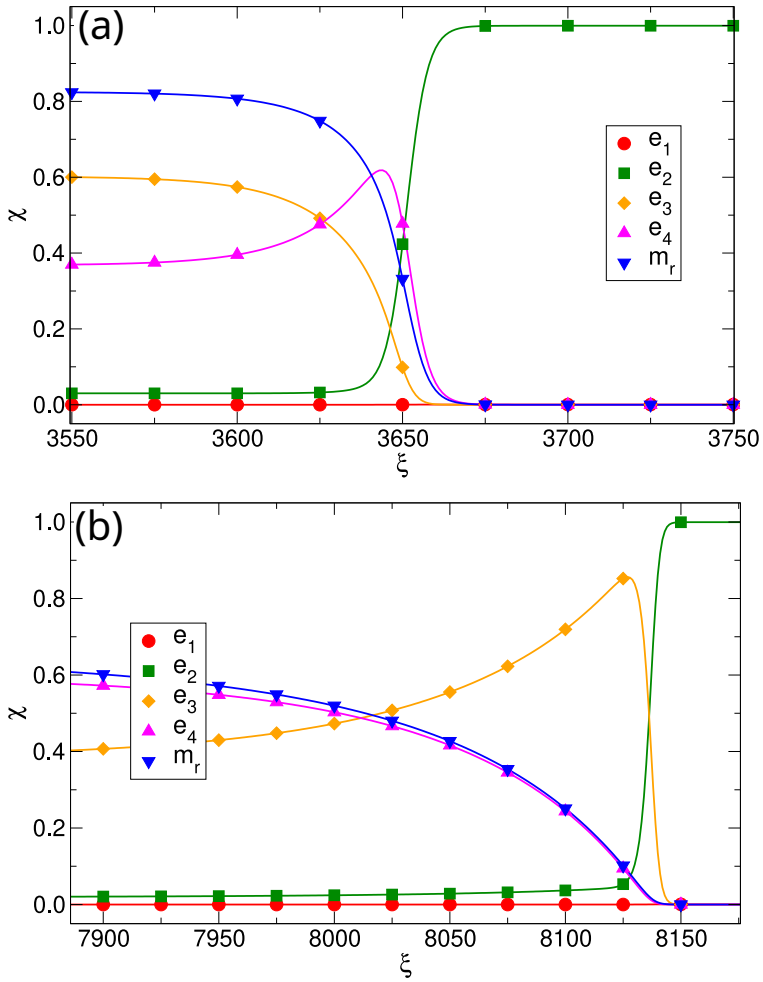

Figure 2: The front profiles obtained at R = 3.5×10^5 (a) and R = 2.5×10^3 (b) ratios. Dimensionless ●: free enzyme concentration (e_1); ■: totally reduced enzyme concentration (e_2); ♦: autocatalytic conformer concentration (e_3); ▲: partially oxidized enzyme concentration (e_4); ▼: reduced electron acceptor concentration (m_r).

II. *The hydrolysis of the Schiff bases we investigated is autocatalytic and in the empirical rate equation the exponent of the autocatalyst concentration* ***n*** *in both cases is around 0.5, which corresponds to parabolic autocatalysis* [2].

During hydrolysis, we recorded the pH changes of two imines labelled with „A" and „B" over time, resulting in the formation of a corresponding aldehyde and amine (Fig.3).

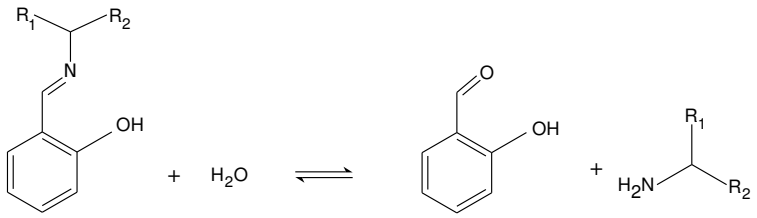

Figure 3: The net reaction of imine hydrolysis. Imine "A": R_1: -H and R_2: -CH_2OH; imine "B": R_1: -CH_3 and R_2: -CH_3.

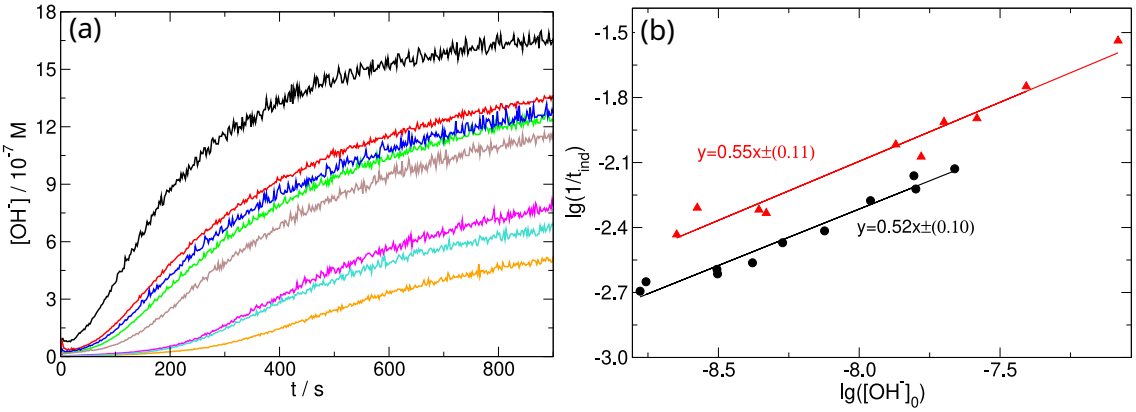

Figure 4: (a): The concentration of hydroxide ion plotted against time in the reaction of imine "A" at different initial pH (b): The logarithm of the reciprocal of the induction times for reactions initiated from different initial pH as a function of the logarithm of the initial hydroxide ion concentration for imine "A" (▲) and "B" (●).

In the experiments, the reaction was initiated from different initial pH (Fig. 4. (a)), which was adjusted by the addition of hydrochloric acid. It can be seen that the lower the initial pH, the longer the reaction induction time, which is inversely proportional to the reaction rate. This occurs because the addition of acid removes the hydroxide ion, the autocatalyst of the reaction. The induction time was determined from the intersection of two straight lines to the initial lag period and the increasing part of the curve. Plotting the logarithm of the reciprocal of the induction times as a function of the logarithm of the initial hydroxide ion concentration, the slope of the fitted line to the resulting points provided the exponent of autocatalysis for both Schiff bases tested (Fig. 4. (b)).

III. *By using the experimental data of hydroxide ion-catalysed autocatalytic hydrolysis of Schiff bases, a model is developed, which occurs when the amine formed in the process is stronger base than the imine, and the hydroxide ion-dependent step is also present* [2].

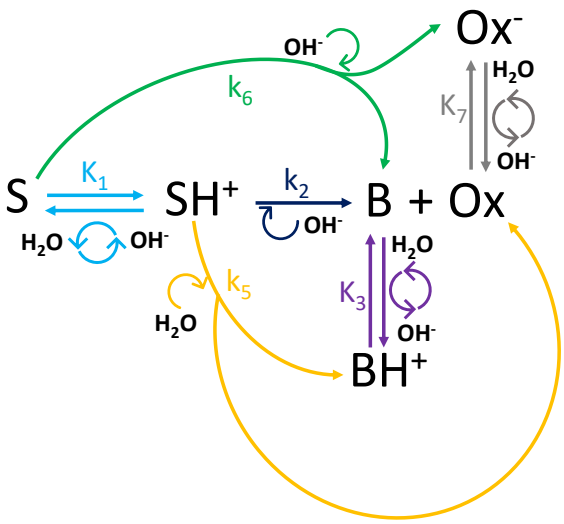

Figure 5: Schematic model of imine hydrolysis. S: Schiff base; SH^+: protonated form of Schiff base; B: amine; BH^+: protonated amine, Ox: aldehyde, Ox^-: phenolate.

It is discovered that hydroxide ion-catalysed autocatalysis occurs in the hydrolysis of Schiff bases when the time evaluation of the hydroxide ion concentration is positive, i.e., this component appears as a product. This observation is supported by the following equation based on the model (Fig. 5.):

$$\frac{dS_T}{dt} = -S_T \frac{K_1 k_5 + K_1 k_2 [\mathrm{OH}^-] + k_6 ([\mathrm{OH}^-])^2}{K_1 + [\mathrm{OH}^-]} \tag{4}$$

$$\frac{d[\mathrm{OH}^-]}{dt} = \frac{\left(\frac{(K_1 - K_3)[\mathrm{OH}^-]}{(K_1 + [\mathrm{OH}^-])(K_3 + [\mathrm{OH}^-])} + \frac{[\mathrm{OH}^-]}{K_7 + [\mathrm{OH}^-]}\right)\frac{dS_T}{dt}}{1 + \frac{K_1 S_T}{(K_1 + [\mathrm{OH}^-])^2} + \frac{K_3 B_T}{(K_3 + [\mathrm{OH}^-])^2} + \frac{K_w}{([\mathrm{OH}^-])^2} + \frac{K_7 Ox_T}{(K_7 + [\mathrm{OH}^-])^2}}. \tag{5}$$

If K_3, the dissociation constant of the amine is greater than K_1, the dissociation constant of the imine, $\frac{d[\mathrm{OH}]^-}{dt}$ is positive, since $\frac{dS_T}{dt}$ is always negative. The hydroxide-ion-dependent step (k_6) only evolves if the hydroxide ions are able to perform a nucleophilic attack against the Schiff base provided by an intramolecular hydrogen bridge.

IV. *For the Schiff bases exhibiting autocatalysis, bistability is possible in an open system, and its occurrence and extent depend on the strength of the non-catalysed (k_5) and the removal step (k_r)* [1].

We have shown in an open system that the appearance of bistability and the extent of the bistable region during hydrolysis of Schiff bases depend on the values of the rate coefficient of the non-catalysed step (k_5) and the rate coefficient of the removal step (k_r) as summarized in Fig. 6. If we plot the rate coefficients of the removal step (k_r) belonging to the saddle-node bifurcation points as the function of flow rate (k_0), we obtain the area bounded by a solid line, the bistable region. As it is outlined in Fig. 6., the larger the contribution of the non-catalysed reaction is, the smaller the range is, and the stronger the abstraction step is, the smaller the contribution of the allowed non-catalysed reaction in the system is.

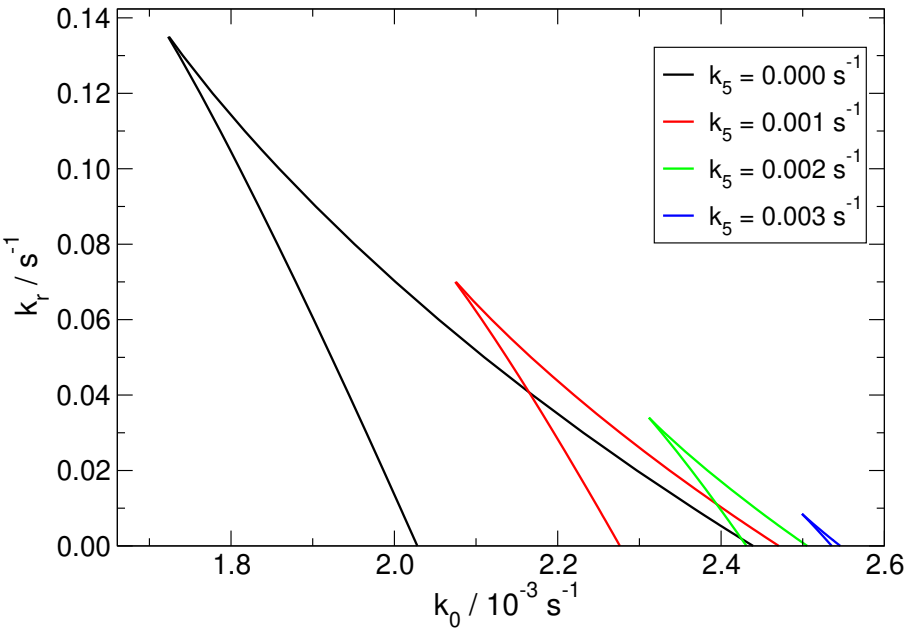

Figure 6: The rate coefficient of the removal step (k_r) against the flow rate (k_0) for different values of non-catalysed rate coefficient (k_5).

V. *The diverse dynamics of the reaction network based on imine hydrolysis is governed by the two largest eigenvalues obtained by linear stability analysis and the ranges of bistability and oscillation in the removal step (k_r) – flow rate (k_0) parameter plane form a cross-shaped diagram* [1].

The complexity of the imine hydrolysis-based reaction network results in complex dynamics, which can be illustrated on the phase diagram composed of the rate coefficient of the removal step (k_r) and the flow rate (k_0). The bistable zone and oscillation range arising from the complex dynamics form a cross-shaped diagram in the $k_r - k_0$ parameter plane, which is represented in Fig. 7. (a) complemented by the different types of bifurcations (subcritical/supercritical Hopf, saddle-loop, double-loop and saddle-loop bifurcations).

The dynamics of the reaction network is determined by the two largest eigenvalues of the Jacobian matrix obtained by linear stability analysis, since all others take negative values over the whole parameter range. Hence, the reaction network can be treated analogously to the two-variable system: the sum of the two eigenvalues can be plotted on the x-axis, while their product can be plotted on the y-axis (7. (b)). The former corresponds to the trace of the Jacobian matrix of the two-variable system and the latter to its determinant.

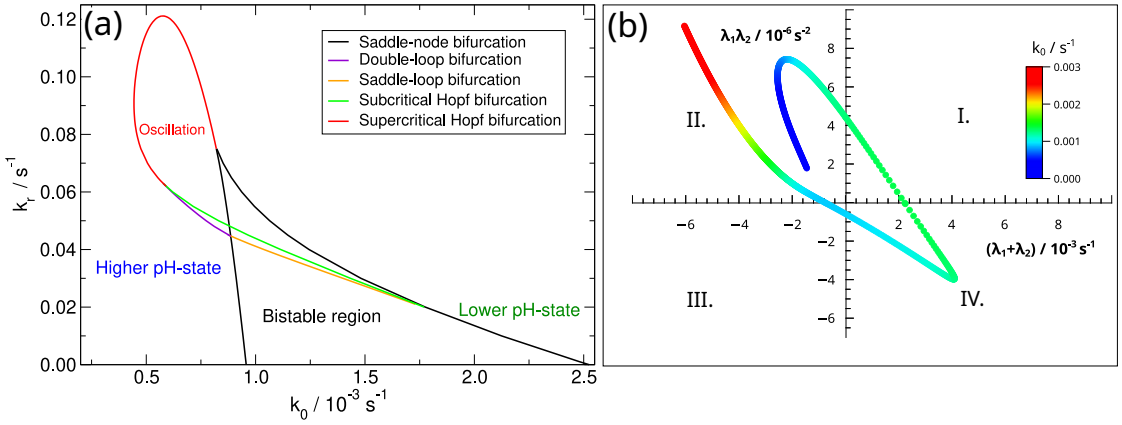

Figure 7: The cross-shaped diagram in the $k_r - k_0$ parameter plate composed of the ranges of bistability and oscillation complemented by the bifurcations (a). Analogous representation of the two eigenvalues of the Jacobian matrix affecting the dynamics of the reaction network to the two-variable systems with the corresponding k_0 values (b).

In Fig. 7. (b), the intersection of the curve and the x-axis provides the saddle-node bifurcation, while the intersection of the curve and the y-axis provides the Hopf bifurcation. As the flow rate decreases, while moving from the red to the blue markers, stable focus/node points appear in the reaction network in the second quadrant, saddle points in the third and fourth quadrants, while unstable node/focus points appear in the first quadrant.

VI. *The reaction network based on imine hydrolysis exhibits oscillation for a suitable parameter set, with amplitude and period influenced by the flow rate (k_0), the rate coefficient of the non-catalysed step (k_5), the rate coefficient of the removal step (k_r) and the protonation equilibrium constant of Schiff base (K_1)* [1].

By increasing the protonation equilibrium constant of Schiff base (K_1), the range of oscillation shifts towards the smaller flow rate values, while increasing the rate coefficient of the non-catalysed reaction (k_5) leads to the shift towards bigger k_0 values. In all cases, the amplitude varies between 0.2 and 2 pH units. As for the contribution of the removal step, the amplitude decreases with increasing k_r. The time period is always in the range of hours, and it increases with increasing the contribution of the removal step. The effect of the flow rate on the amplitude and time period is illustrated in Fig. 8., which shows that increasing k_0 within this range increases threefold the time period, but does not affect the amplitude significantly.

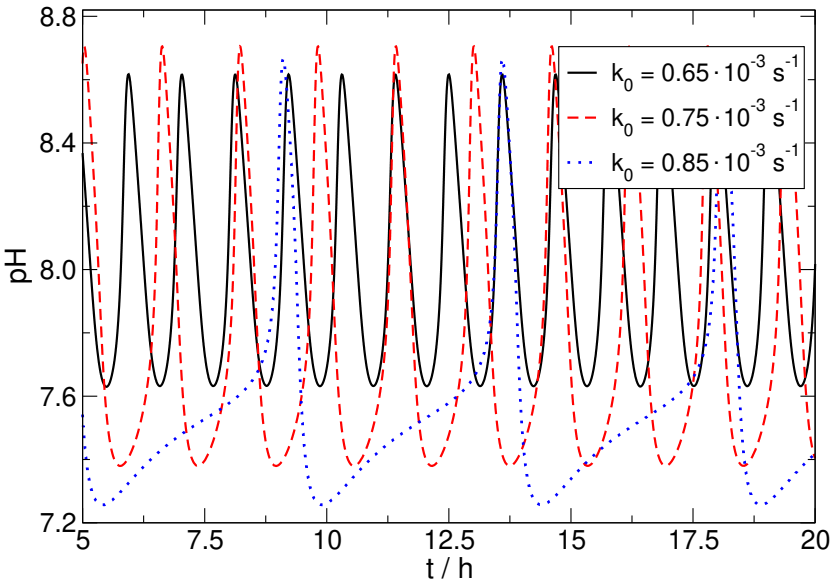

Figure 8: The effect of flow rate (k_0) on the amplitude and time period of oscillation.

5 List of Scientific Publications

5.1 Scientific Publications Related to the Topic of the Dissertation

1. **E. Lantos**, Á. Tóth, D. Horváth

   Oscillatory dynamics in a reaction network based on imine hydrolysis

   Chaos, **33**, 103104 (2023)

   https://doi.org/10.1063/5.0169860

   IF_{2022} = 2.9 (Q1)

2. **E. Lantos**, G. Mótyán, É. Frank, R. Eelkema, J. van Esch, D. Horváth, Á. Tóth

   Dynamics of hydroxide-ion-driven reversible autocatalytic networks

   RSC Adv., **13**, 20243-20247 (2023)

   https://doi.org/10.1039/D3RA04215D

   IF_{2022} = 3.9 (Q2)

3. L. Gyevi-Nagy **E. Lantos**, T. Gehér-Herczegh, Á. Tóth, Cs. Bagyinka, D. Horváth

   Reaction fronts of the autocatalytic hydrogenase reaction

   J. Chem. Phys., **148**, 165103 (2018)

   https://doi.org/10.1063/1.5022359

   IF_{2018} = 2.997 (Q1)

   $\sum$IF = 9.797

5.2 Other Scientific Publications

1. R. Zahorán, P. Kumar, Á. Deák, **E. Lantos**, D. Horváth, Á. Tóth

   From balloon to crystalline structure in the calcium phosphate flow-driven chemical garden

   Langmuir, **39**, 5078–5083 (2023)

   https://doi.org/10.1021/acs.langmuir.3c00079

   IF_{2022} = 3.9 (Q1)

2. M. Emmanuel, **E. Lantos**, D. Horváth, Á. Tóth

   Formation and growth of lithium phosphate chemical gardens

   Soft Matter, **18**, 1731–1736 (2022)

   https://doi.org/10.1039/D1SM01808F

   IF_{2022} = 3.4 (Q1)

3. Á. Tóth, G. Schuszter, N. P. Das, **E. Lantos**, D. Horváth, A. De Wit, F. Brau

   Effects of radial injection and solution thickness on the dynamics of confined A plus B -> C chemical fronts

   Phys. Chem. Chem. Phys., **22**, 10278–10285 (2020)

   `https://doi.org/10.1039/C9CP06370F`

   IF_{2020} = 3.676 (Q1)

4. **E. Lantos**, L. Mérai, Á. Deák, J. Gómez-Pérez, D. Sebők, I. Dékány, Z. Kónya, L. Janovák

   Preparation of sulfur hydrophobized plasmonic photocatalyst towards durable superhydrophobic coating material

   J. Mater. Sci. Technol., **41**, 159–167 (2020)

   `https://doi.org/10.1016/j.jmst.2019.04.046`

   IF_{2020} = 8.067 (D1)

5. **E. Lantos**, N. P. Das, D. S. Berkesi, D. Dobó, Á. Kukovecz, D. Horváth, Á. Tóth

   Interaction between amino-functionalized inorganic nanoshells and acid-autocatalytic reactions

   Phys. Chem. Chem. Phys., **20**, 13365–13369 (2018)

   `https://doi.org/10.1039/c8cp01053f`

   IF_{2018} = 3.567 (Q1)

$\sum$IF = 22.61

6 Lectures

6.1 Lectures Related to the Topic of the Dissertation

1. **Emese Lantos**, Dezső Horváth, Ágota Tóth

   Autocatalytic reaction networks in bioinspired systems

   Preliminary presentation of dissertation, Reaction Kinetics and Photochemistry Working Group of HSA, June 8-9, 2023; Balatonvilágos, Hungary

2. **Emese Lantos**, Dezső Horváth, Ágota Tóth

   The modelling of a pH oscillator based on imine hydrolysis

   Reaction Kinetics and Photochemistry Working Group of HSA, October 27-28, 2022; Balatonvilágos, Hungary (online)

3. **Emese Lantos**, Ágota Tóth, Dezső Horváth

   Oscillations and bistability in the autocatalytic reaction network of imine hydrolysis

   Dynamics Days Europe, August 22-26, 2022; Aberdeen, Scotland

4. **Emese Lantos**, Dezső Horváth, Ágota Tóth

   The modelling of hydroxide ion-driven autocatalytic reaction networks

   Seminar at the Department of Physical Chemistry and Materials Science, University of Szeged, May 17, 2022; Szeged, Hungary

5. **Emese Lantos**, Dezső Horváth, Ágota Tóth

   Dynamics of Hydroxide-Ion-driven Reversible Autocatalytic Networks

   15th International Conference on Fundamental and Applied Aspects of Physical Chemistry, September 20-24, 2021; Belgrade, Serbia (online)

6. **Lantos Emese**, Horváth Dezső, Tóth Ágota

   The design of hydroxide ion-driven autocatalytic reaction networks

   Physical Chemistry and Materials Science Working Group of ACSz, June 8, 2021; Szeged, Hungary (online)

7. **Emese Lantos**, Dezső Horváth, Ágota Tóth

   Dynamics of Hydroxide-Ion-driven Reversible Autocatalytic Networks

   Chemical Systems Meeting, March 22-23, 2021 (online)

8. **Emese Lantos**, Dezső Horváth, Ágota Tóth

   Towards designing imine-based oscillators: autocatalytic hydrolyses of imines

   XLII. Chemistry Lectures, October 28-30, 2019; Szeged, Hungary

9. **Emese Lantos**, Dezső Horváth, Ágota Tóth

   The design of organic oscillator

   Reaction Kinetics and Photochemistry Working Group of HSA, May 23-24, 2019; Balatonalmádi, Hungary

10. **Lantos Emese**, Tóth Ágota, Horváth Dezső

    The autocatalytic hydrolysis of imines

    XLI. Chemistry Lectures, October 15-17, 2018; Szeged, Hungary

11. Dezső Horváth László Gyevi-Nagy, **Emese Lantos**, Ágota Tóth

    Reaction-diffusion fronts driven by the autocatalytic hydrogenase reaction

    14th International Conference on Fundamental and Applied Aspects of Physical Chemistry, September 24-28, 2018; Belgrade, Serbia

12. László Gyevi-Nagy, **Emese Lantos**, Ágota Tóth, Dezső Horváth

    Modelling the hydrogenase front reaction

    Reaction Kinetics and Photochemistry Working Group of HSA, November 3-4, 2016; Mátraháza, Hungary

13. László Gyevi-Nagy, **Emese Lantos**, Ágota Tóth, Dezső Horváth

    Modelling the hydrogenase front reaction

    XXIX. Chemistry Lectures, October 17-19, 2016; Szeged, Hungary

14. Tünde Gehér-Herczegh, **Emese Lantos**, Csaba Bagyinka, Ágota Tóth, Dezső Horváth

    Spatio-temporal pattern formation in an autocatalytic hydrogenase reaction

    Conference SysChem 2016, CMST COST Action, May 5-12, 2016; Valtice, Czech Republic

15. Tünde Herczegh, **Emese Lantos**, Csaba Bagyinka, Ágota Tóth, Dezső Horváth

    Spatio-temporal pattern formation in an autocatalytic hydrogenase reaction

    Beyond Self Assembly Workshop, January 21-24, 2016; Bad Gastein, Austria

6.2 Other Lectures

1. Ágota Tóth, Gábor Schuszter, Nirmali Prabha Das, **Emese Lantos**, Dezső Horváth, Ann De Wit, Fabian Brau

   Dynamics of radially propagating chemical fronts

   Reaction Kinetics and Photochemistry Working Group of HSA, November 7-8, 2019; Mátrafüred, Hungary

2. **Lantos Emese**, Nirmali Prabha Das, Tóth Ágota, Horváth Dezső

   Interaction between autocatalytic chemical reaction and inorganic nanospheres

   XL. Chemistry Lectures, October 16-18, 2017; Szeged, Hungary

7 Posters

7.1 Poster Presentations Related to the Topic of the Dissertation

1. **Emese Lantos**, Stevan Macesic, Ágota Tóth, Dezső Horváth

   Spatiotemporal dynamics of autocatalytic reversible reaction networks

   GRC Systems Chemistry, June 26 - July 1, 2022; Newry, USA

2. **Emese Lantos**, Dezső Horváth, Ágota Tóth

   Spatiotemporal patterns in the autocatalytic hydrogenase reaction

   Systems Chemistry Virtual Symposium, July 7-9, 2021, online

7.2 Other Poster Presentations

1. Nirmali Prabha Das, **Emese Lantos**, Dezső Horváth, Ágota Tóth

   Coupling of self-assembly and self-organization of different length scales

   GRC on Systems Chemistry, July 29 - August 3, 2018; Newry, USA

2. Nirmali Prabha Das, **Emese Lantos**, Dezső Horváth, Ágota Tóth

   Coupling of self-assembly and self-organization of different length scales

   GRC on Oscillations and Dynamic Instabilities in Chemical Systems, July 8-13, 2018; Les Diablerets, Switzerland

MTMT identification number: 10069335